energies

MDPI

Article

Determination of Pressure Drop Correlation for Air Flow through Packed Bed of Sinter Particles in Terms of Euler Number

Junsheng Feng [1], Liang Zhao [2], Haitao Wang [1], Zude Cheng [1], Yongfang Xia [1,*] and Hui Dong [2]

[1] School of Environment and Energy Engineering, Anhui Jianzhu University, Hefei 230601, China; fjsheng@ahjzu.edu.cn (J.F.); wht@ahjzu.edu.cn (H.W.); czd@ahjzu.edu.cn (Z.C.)
[2] School of Metallurgy, Northeastern University, Shenyang 110819, China; zhaoliang1@mail.neu.edu.cn (L.Z.); dongh@smm.neu.edu.cn (H.D.)
* Correspondence: xiayf@ahjzu.edu.cn; Tel.: +86-551-6382-8252

Abstract: In order to clearly understand the air flow resistance characteristics in vertical tanks for sinter waste heat recovery in the steel industry, experimental research on the air flow pressure drop (FPD) performance in a sinter bed layer (BL) was conducted. Based on a self-made experimental device, the measurement values of air FPD for different experimental conditions were determined firstly, and then the concept of Euler number (Eu) in heat exchangers was introduced into the study of air FPD in BL; the change rules of *Eu* under different particle diameters were analyzed. Finally, the air FPD correlation in sinter BL was obtained and described in the form of *Eu*, and the error analysis of obtained air FPD correlation was performed. The results show that, the air FPD increases as a second power relationship with the increase in air superficial velocity when the particle diameter is constant. The decrease amplitude of *Eu* gradually dwindles when increasing the Reynolds number (*Re*), and the decrease in the *Eu* shows a reciprocal relationship with the *Re*. As the bed geometry factor increases, the FPD coefficient, *A*, decreases as an exponential relationship, while the FPD coefficient, *B*, increases as a first power relationship. The obtained air FPD correlation in the form of *Eu* in the experiment is well compatible with the measurement values, and the mean deviation of obtained correlation is 4.67%, showing good originality.

Keywords: sinter; packed bed; pressure drop; Euler number; Reynolds number

Citation: Feng, J.; Zhao, L.; Wang, H.; Cheng, Z.; Xia, Y.; Dong, H. Determination of Pressure Drop Correlation for Air Flow through Packed Bed of Sinter Particles in Terms of Euler Number. *Energies* **2022**, *15*, 4034. https://doi.org/10.3390/en15114034

Academic Editors: Katarzyna Antosz, Jose Machado, Yi Ren, Rochdi El Abdi, Dariusz Mazurkiewicz, Marina Ranga, Pierluigi Rea, Vijaya Kumar Manupati, Emilia Villani and Erika Ottaviano

Received: 25 March 2022
Accepted: 24 May 2022
Published: 31 May 2022

1. Introduction

Packed beds are widely used in the metallurgical industries as the heat exchangers and high temperature gas-cooled reactors [1–3], which have gained popularity because of the convenience of operation and low cost. A lot of researchers have been commissioned to investigate the mechanisms of fluid flow and heat transfer in packed beds, and it is still in progress [4].

The sinter vertical tank (SVT) is high-efficient recovery equipment of sinter waste heat [5,6], which is aimed to overcome the shortcomings of existing waste heat recovery equipment [7]. In essence, the bed layer (BL) with sinter particles in SVT is a kind of random packed bed, and the air flow pressure drop (FPD) in SVT affects the required power of the air blower, and then affects the economic feasibility of SVT. Therefore, it is of great significance to study the air FPD characteristics in SVT for improving the sinter waste heat recovery rate and analyzing the economic feasibility of SVT.

Understanding the fluid FPD performance in a packed bed is very important as it affects the required power of pump and blower in actual applications. There have been many pieces of research on the fluid FPD performance in particle-packed beds in the last few decades [8–18]. Montillet [8] experimentally studied the fluid FPD behavior in a packed bed with spheres under different Reynolds number (*Re*) and bed geometry factor (D/d_p), and the

values of fluid FPD in the central region of the packed bed were measured. Yang et al. [10] investigated the fluid FPD behavior in structured packed beds by experimental and numerical methods. Bu et al. [12] numerically investigated the fluid FPD behavior in structured packed beds with particles by using different treatment methods. Tian et al. [14] experimentally investigated the FPD characteristics in structured BL with spheres and determined the quantitative relationship of FPD with flow velocity. Halkarni et al. [16] studied the effect of D/d_p on FPD in randomly packed beds with uniform-sized spherical particles, and the measured friction factor compared reasonably with the available correlations in the literature. Toit et al. [18] investigated the FPD behavior in packed beds and performed an evaluation of the friction factors as a function of the modified *Re* for the FPD through randomly and structured packed beds consisting only of uniform-sized spheres.

Except for the above studies of fluid FPD performance in packed beds, the studies of FPD correlation in particle packed beds have also been conducted by lots of researchers [19–30]. The well-known Ergun's equation [19] applied to describe the fluid FPD in packed beds is shown in Equation (1).

$$\frac{\Delta P}{H} = 150\frac{\mu(1-\varepsilon)^2}{\varepsilon^3 {d_p}^2}u + 1.75\frac{\rho(1-\varepsilon)}{\varepsilon^3 d_p}u^2 \quad (1)$$

The first and second terms in Equation (1) are the laminar and turbulent components, respectively, and the corresponding coefficients (150, 1.75) are the viscous and inertial resistance coefficients. Due to the difference of particle size and shape in packed beds, the equation coefficients (150, 1.75) have been modified for predicting the FPD in various particle packed beds by some other researchers. Macdonald et al. [20] experimentally gave the modified coefficients of 180 and 1.8. Meanwhile, Comiti and Renaud [21] and Ozahi et al. [22] also experimentally presented their modified coefficients, namely the coefficients (141, 1.63) and coefficients (160, 1.61). Dukhan et al. [23] and Amiri et al. [24] also experimentally obtained the algebraic values of modified coefficients, which are all the interval range values. In addition to this, there is another indirect expression for describing the fluid FPD in particle packed beds, namely the friction factor, the definition of which is given as follows.

$$f_p = \frac{\Delta P d_p}{H\rho u^2} \quad (2)$$

Based on the definition of f_p proposed by Kürten et al. [25] and Hicks [26], they are valid in the range of $0.1 \leq Re \leq 4000$ and $500 \leq Re \leq 60{,}000$. Meanwhile, the correlations of f_p are obtained by Tallmadge [27] and Lee and Ogawa [28] with a large range of $0.1 \leq Re \leq 100{,}000$ and $1 \leq Re \leq 100{,}000$. In all of the above correlations, f_p are defined as a function of *Re* and BL voidage (ε) only. Furthermore, Montillet et al. [29] and Özahi et al. [30] experimentally obtained the correlations of f_p with the range of $10 \leq Re \leq 2500$ and $708 \leq Re \leq 7772$, and except for *Re* and ε, the D/d_p is also considered in their correlations.

The above studies on packed beds mostly focused on the FPD performance and correlation correction of FPD in BL with uniform-sized particles. Nevertheless, there was a great difference in the fluid FPD for different particle size and shape in packed beds. In addition, the existing fluid FPD correlations in particle-packed beds were mainly in the form of Ergun's equation and f_p, while the FPD correlation in the form of Euler number (*Eu*) only appeared in the study of FPD in heat exchangers [31–33]. Based on an authors' literature survey, there is almost no research to investigate the fluid FPD correlation in the form of *Eu* in particle-packed beds.

To sum up, the concept of *Eu* in heat exchangers was introduced into the fluid FPD research in particle BL, and the air FPD performance in sinter BL was restudied and analyzed through the *Eu* method in this paper by using the experimental data shown in our previous research [34]. Firstly, the measurement values of air FPD for different experimental conditions were obtained, according to the experimental data shown in our previous research [34],

and then the change relationships between *Eu* and *Re* under different particle diameters were determined. Finally, the FPD correlation in the form of *Eu* in sinter BL was defined, and the applicability of FPD correlation obtained under different experimental conditions was also analyzed. The FPD correlation in the form of *Eu* related to air FPD characteristics will provide a theoretical reference in sinter BL for industrial applications.

2. Experimental Device and Process

The self-made experimental device shown in our previous research [34] was presented in Figure 1. The experimental device was mainly composed of four parts: an air blower to drive the air flow through the sinter BL, a throttle valve to adjust the air flow rate, an orifice plate flowmeter to display the specific size of the air flow rate, and a vertical device with three pressure measuring holes to measure the air FPD at different BL heights. The inner diameter of the vertical device was 430 mm, and three pressure measuring holes installed at different vertical locations (400 mm, 700 mm and 1200 mm) were applied to measure the air FPD in sinter BL.

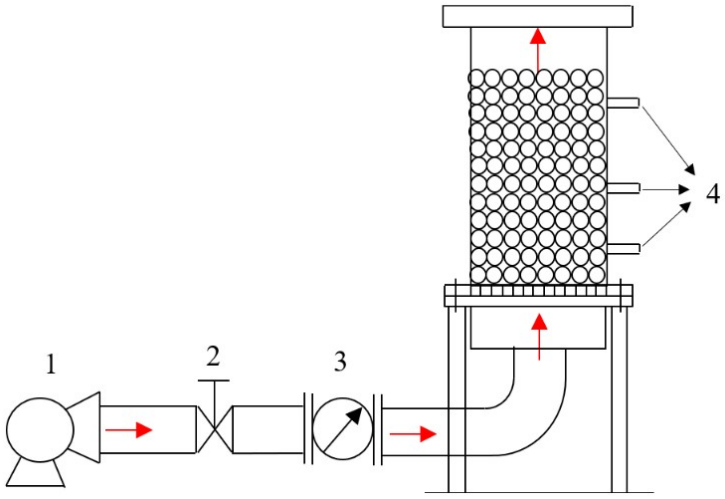

Figure 1. Schematic diagram of air flow experimental device: 1. Air blower, 2. Throttle valve, 3. Orifice plate flowmeter, 4. Pressure measuring holes.

Because of the inhomogeneity of sinter particles, the standard test sieves of different sizes were applied to sieve out the all sizes of sinter particles, and three kinds of sieved particle diameters with 14 mm, 24 mm and 35 mm were used in the experiment, shown in Table 1. The particle sphericity (Φ) was obtained through the gas flow technique [35]. The particle equivalent diameter (d_p) was the product of sieved particle diameter and particle sphericity, and the D/d_p was the ratio of inner diameter of experimental cylinder to particle equivalent diameter. The rated flow of the air blower was 1650 m^3/h, and the experimental conditions were conducted with the air flow rate range of 200~1600 m^3/h under the normal condition of T_0 = 293.15 K.

Table 1. Related parameters of sinter particles.

d (mm)	Φ	d_p (mm)	D/d_p
14	0.69	9.66	44.5
24	0.72	17.28	24.9
35	0.89	31.15	13.8

The experimental values of air FPD per unit height, $\Delta P(r)/H$, along the radial direction of sinter BL were calculated and determined for different BL heights by taking the differences of pressure values at measurement points firstly, and then the average values

of FPD per unit height ($\Delta P/H$) along the radial direction for different BL heights were obtained under different particle diameters and air flow rates. Subsequently, according to the average values along the radial direction for different BL heights, the changes of mean $\Delta P/H$ with the air superficial velocity for different particle diameters were determined, and the relationships between *Eu* and *Re* under different particle diameters were also obtained. Finally, the FPD correlation in the form of *Eu* was defined through the method of data regression analysis, and the error analysis of obtained FPD correlation was also performed.

3. Results and Discussion

3.1. Measurement of Air FPD

Along the radial direction of sinter BL, the locations of six measurement points are identified, and the *r*/*R* for different locations are 0, 0.2, 0.4, 0.6, 0.8 and 0.96, respectively. Among the *r*/*R*, *r* is the actual distance between the measured point and the center of BL, and *R* is the radius of BL. The purpose of this measurement operation is to overcome the influences of particle inhomogeneity and the wall effect of BL on the air FPD. The measurement values of $\Delta P(r)/H$ at six measurement points is used to calculate the average value of $\Delta P/H$ along the radial direction for a given experimental condition, and according to the experimental data of air FPD shown in our previous research [34], the changes of $\Delta P/H$ with the air flow rate under different BL heights and particle diameters are shown in Figure 2. It can be seen from Figure 2, the $\Delta P/H$ increases with the increase in air flow rate, and the increase amplitude of $\Delta P/H$ is getting larger and larger. This may be explained that the increase in air flow rate results in the air superficial velocity, and based on Equation (1), the $\Delta P/H$ in sinter BL is proportional to the quadratic power of superficial velocity, which leads to the larger increase amplitude of $\Delta P/H$ shown in Figure 2.

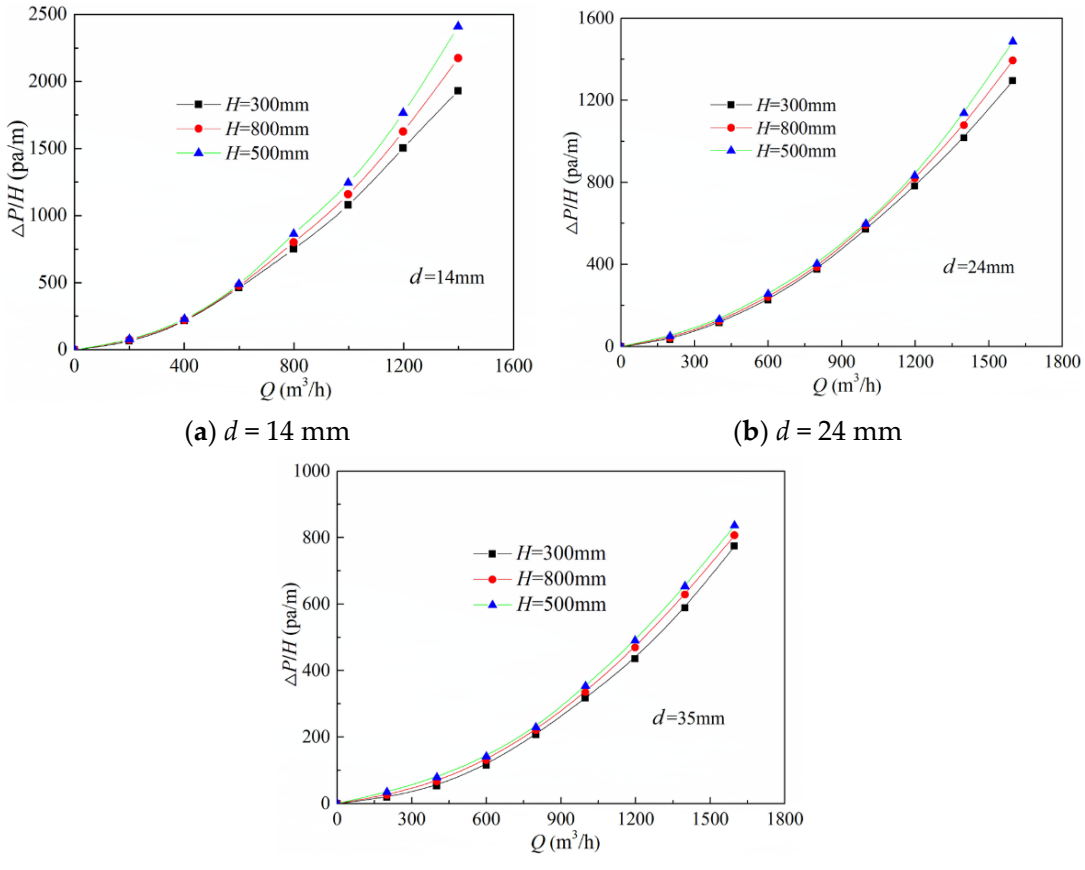

(**a**) d = 14 mm (**b**) d = 24 mm

(**c**) d = 35 mm

Figure 2. Changes of $\Delta P/H$ with Q under different BL heights and particle diameters [34].

In addition, Figure 2 also shows that the values of $\Delta P/H$ are different for various BL heights when the particle diameter is constant, the $\Delta P/H$ for the BL height of 300 mm (400–700 mm) is the smallest, and the $\Delta P/H$ for the BL height of 800 mm (400–1200 mm) is middle, while the $\Delta P/H$ for the BL height of 500 mm (700–1200 mm) is the largest. The result may be because of the difference of packing structure of sinter particles in BL, the particle size at the bottom of BL is relatively larger than that at the top of BL, which results in the smaller ε at the top of BL, so the $\Delta P/H$ at the top of BL is relatively larger.

Based on the above measurement values of $\Delta P/H$ for different BL heights, the changes of mean $\Delta P/H$ with air superficial velocity under three particle diameters are listed in Figure 3, which is taken from our previous research [34]. As known from Figure 3, the increase in $\Delta P/H$ shows a second power relationship as the air superficial velocity increases, and the $\Delta P/H$ decreases as the particle diameter increases when the air superficial velocity is constant. This may be explained by considering that the ε increases as the particle diameter increases, and both the viscous and inertial resistances of air flow through the BL will decrease, which leads to the decrease in $\Delta P/H$.

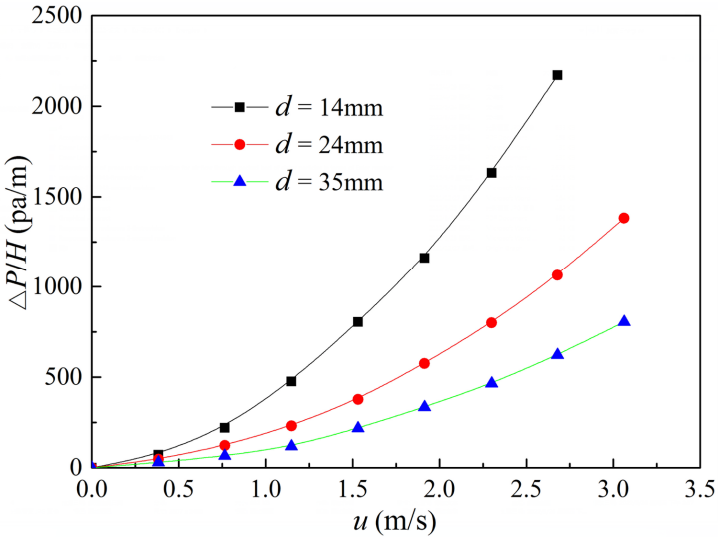

Figure 3. Changes of mean $\Delta P/H$ with u under different particle diameters.

3.2. Analysis of Eu–Re Relationship

As known from the above literatures [19–24], the general correlation of Ergun's equation can be described as follows.

$$\frac{\Delta P}{H} = k_1 \frac{\mu(1-\varepsilon)^2}{\varepsilon^3 {d_p}^2} u + k_2 \frac{\rho(1-\varepsilon)}{\varepsilon^3 d_p} u^2 \tag{3}$$

where k_1 is the coefficient of viscosity resistance, and k_2 is the coefficient of inertia resistance.

According to the definition of Eu, the expression of Eu is given below, which reflects the relative relationship of FPD in flow field with dynamic pressure.

$$Eu = \frac{\Delta P}{\rho u^2} \tag{4}$$

Through the combination of Equations (3) and (4), the Eu used to describe the fluid FPD in particle BL is determined below.

$$Eu = H\left[k_1 \frac{\mu(1-\varepsilon)^2}{\rho \varepsilon^3 {d_p}^2 u} + k_2 \frac{(1-\varepsilon)}{\varepsilon^3 d_p}\right] \tag{5}$$

$$Eu = \frac{H}{D}\left[k_1 \frac{(1-\varepsilon)^2}{\varepsilon^3}\frac{D}{d_p}\frac{1}{Re} + k_2 \frac{(1-\varepsilon)}{\varepsilon^3}\frac{D}{d_p}\right] \tag{6}$$

For a given experimental condition, the ε and D/d_p, as well as the coefficients k_1 and k_2 are constant, so Equation (6) can be modified to the following form.

$$Eu = \frac{H}{D}\left(\frac{A}{Re} + B\right) \tag{7}$$

where A and B are the correlation coefficients, which can be written below, respectively.

$$A = k_1 \frac{(1-\varepsilon)^2}{\varepsilon^3}\frac{D}{d_p} \tag{8}$$

$$B = k_2 \frac{(1-\varepsilon)}{\varepsilon^3}\frac{D}{d_p} \tag{9}$$

Based on the measurement values of $\Delta P/H$ under the different particle diameters mentioned in Figure 3, the changes of Eu with Re under three particle diameters for the BL height of 800 mm are listed in Figure 4. As known from Figure 4, the Eu gradually decreases as the Re increases for the three particle diameters, and the larger is the Re, the smaller is the decrease amplitude of Eu. Through the data fitting, the quantitative relationships of Eu with Re for the three particle diameters are also obtained and listed in Figure 4, and the Eu decreases as a reciprocal relationship with the increase in Re, which is consistent with the analysis of Equation (7).

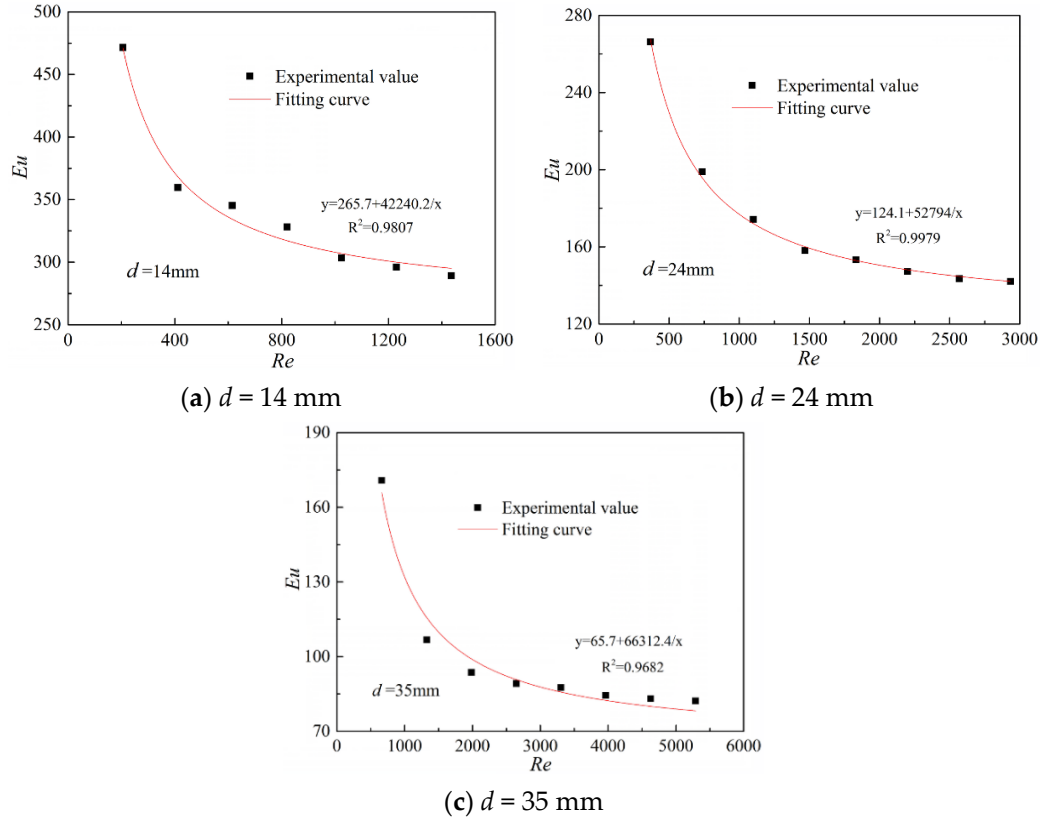

(**a**) d = 14 mm (**b**) d = 24 mm

(**c**) d = 35 mm

Figure 4. Relationships of Eu with Re under different particle diameters.

3.3. Determination of Pressure Drop Correlation

According to the literature [19–30] mentioned above, some FPD correlations in the form of Ergun's equation and f_p have been determined to calculate the $\Delta P/H$ in particle-

packed beds. In order to verify the applicability of the FPD correlations mentioned in the above literatures, four correlations in the form of f_p [25–28] are selected and listed in Table 2, and the ε for the packed beds with particle diameters of 14 mm, 24 mm and 35 mm are 0.44, 0.49 and 0.53, respectively [35]. The comparisons of calculation values of $\Delta P/H$ calculated by the FPD correlations cited in the literature [25–28] and measurement values of $\Delta P/H$ obtained under different experimental conditions are shown in Figure 5. It could be easily obtained from Figure 5, although the correlation cited in the literature [28] fits the measurement values of $\Delta P/H$ for d = 14 mm with a small deviation, and the correlations cited in the literature [26,27] also fit the measurement values of $\Delta P/H$ for d = 35 mm with a small deviation, but according to the whole measurement values of $\Delta P/H$, all of the above selected correlations cited in the literature [25–28] are not suitable for calculating the $\Delta P/H$ in sinter BL.

Table 2. Correlations for fluid FPD in packed bed with particles.

Authors/Reference	Correlation	Range of Validity
Kürten et al. [25]	$f_p = \left[\frac{25(1-\varepsilon)^2}{4\varepsilon^3}\right]\left[21Re^{-1} + 6Re^{-0.5} + 0.28\right]$	$0.1 \leq Re \leq 4000$
Hicks [26]	$f_p = 6.8\frac{(1-\varepsilon)^{1.2}}{\varepsilon^3}Re^{-0.2}$	$500 \leq Re \leq 60000$
Tallmadge [27]	$f_p = 150\frac{(1-\varepsilon)^2}{\varepsilon^3 Re} + 4.2\frac{(1-\varepsilon)^{1.1666}}{\varepsilon^3}Re^{-1/6}$	$0.1 \leq Re \leq 100000$
Sug Lee and Ogawa [28]	$f_p = \frac{1}{2}\left[\frac{12.5(1-\varepsilon)^2}{\varepsilon^3}\right]\left[29.32Re^{-1} + 1.56Re^{-n} + 0.1\right]$ with $n = 0.352 + 0.1\varepsilon + 0.275\varepsilon^2$	$1 \leq Re \leq 100000$

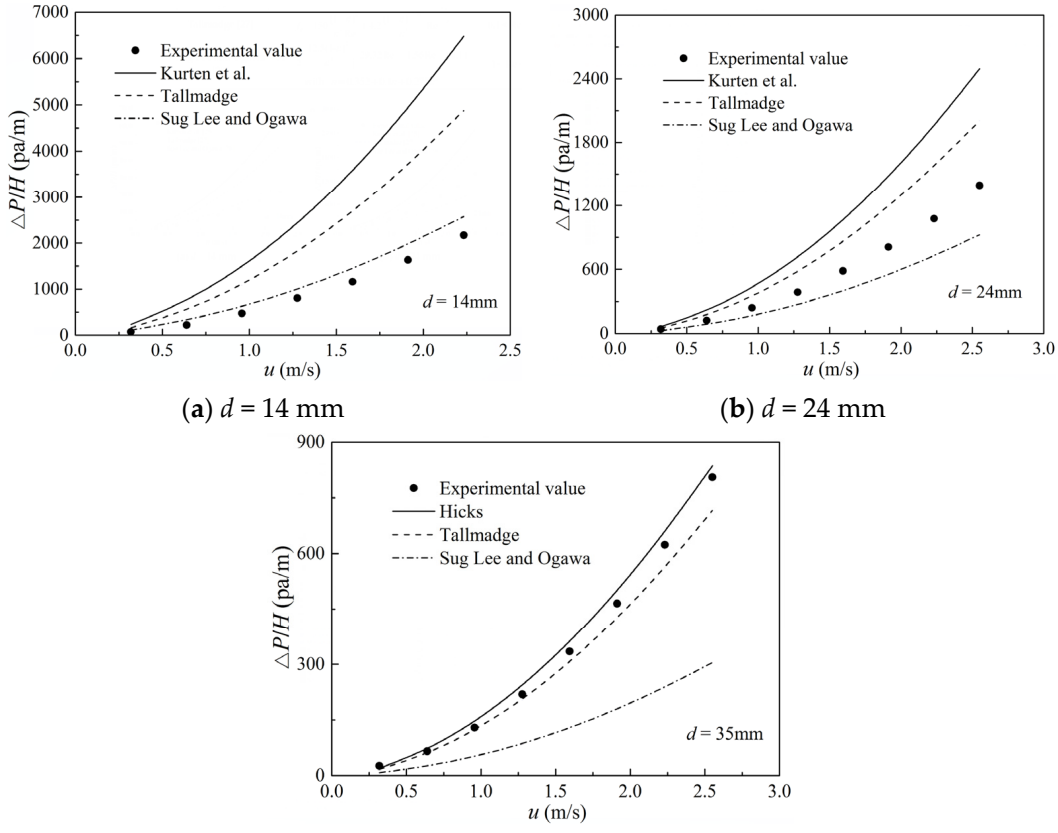

(**a**) d = 14 mm (**b**) d = 24 mm

(**c**) d = 35 mm

Figure 5. Comparisons of calculation and experimental values for different particle diameters.

Based on our previous research results [36], the ε is the function of D/d_p. Therefore, the correlation coefficients, A and B, are also considered as the function of D/d_p. The

quantitative relationships of coefficients A and B with the D/d_p are shown in Figure 6. As known from Figure 6, the coefficient, A, decreases as an exponential relationship with the increasing D/d_p, while the coefficient, B, increases as a first power relationship. Furthermore, the specific relationships of coefficients, A and B, with the D/d_p are given below through the data fitting.

$$A = \left[1.96 + 3.35e^{(-0.053D/d_p)}\right] \times 10^4 \tag{10}$$

$$B = 3.51D/d_p - 16.1 \tag{11}$$

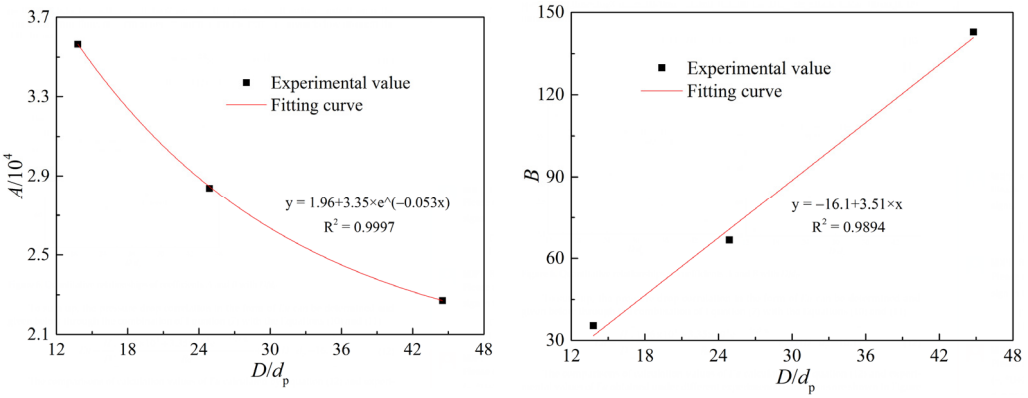

Figure 6. Quantitative relationships of coefficients A and B with D/d_p.

To sum up, the pressure drop correlation in the form of Eu can be determined and given below through the combination of Equation (7) with the Equations (10) and (11).

$$Eu = \frac{H}{D}\left[\frac{1.96 \times 10^4 + 3.35 \times 10^4 e^{(-0.053D/d_p)}}{Re} + 3.51D/d_p - 16.1\right] \tag{12}$$

The comparisons of calculation values of Eu calculated by Equation (12) and experimental values of Eu obtained under different experimental conditions are shown in Figure 7.

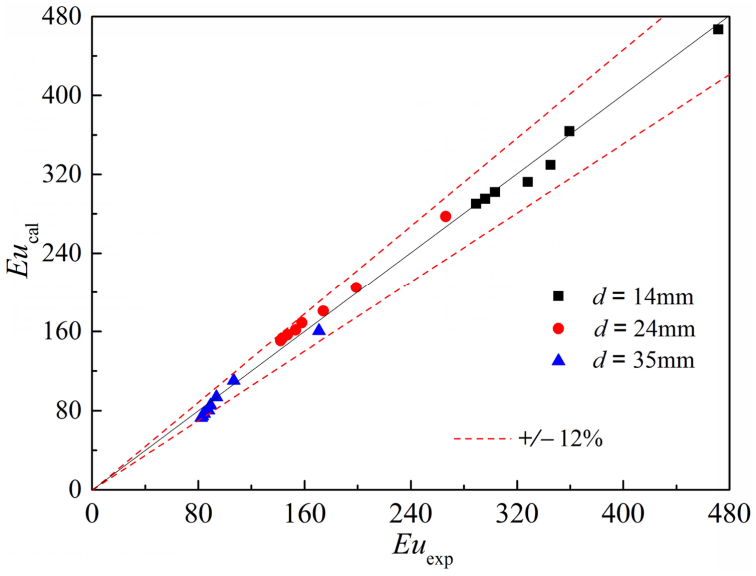

Figure 7. Comparison between experimental values and calculation values of Equation (12).

As easily seen from Figure 7, the calculation values of *Eu* match the experimental values of *Eu* better for various experimental cases. The average deviation of Equation (12) is 4.67%, and the maximum deviation of which is 11.51%, which means that Equation (12) provides a better prediction correlation to calculate the $\Delta P/H$ in sinter BL. Furthermore, compared with the above FPD correlations mentioned in the literature [19,25–28], the component of Equation (12) is relatively simple—only including the effortless calculation factors, namely the height–diameter ratio (*H/D*), *Re* and D/d_p—and shows good originality. In addition, compared with the modified Ergun's correlation in our previous result [34], the average deviation of Equation (12) is basically the same as that of modified Ergun's correlation, but when the inner diameter of the experimental cylinder (*D*) is larger, the applicability of modified Ergun's correlation in our previous result [34] is worse. However, the inner diameter of experimental cylinder has very little effect on the result of the pressure drop correlation in Equation (12). That is why we refit the FPD correlation in particle BL by the *Eu* method, the FPD correlation in the form of Euler number overcomes this problem better.

4. Conclusions

The air FPD performance in sinter BL under different particle diameters is investigated by the experimental method, and the major research results are given below.

(1) The air FPD, $\Delta P/H$, increases as a second power relationship with increasing air superficial velocity when the particle diameter is constant, and the $\Delta P/H$ decreases as the particle diameter increases for a given air superficial velocity.
(2) The *Eu* decreases as the *Re* increases for a given particle diameter, and the decrease in the *Eu* shows a reciprocal relationship with the *Re*. The coefficient, *A*, decreases as an exponential relationship with the increasing D/d_p, while the coefficient, *B*, increases as a first power relationship.
(3) The air FPD correlation in the form of *Eu* is obtained experimentally. Compared with the FPD correlations cited in the previous literature, the obtained correlation in the form of *Eu* match the whole experimental values better, and the average deviation of the obtained correlation is only 4.67%, which shows good originality.

The research result of the present work will provide a theoretical reference for the determination of required air blower power in SVT for industrial applications.

Author Contributions: All authors contributed to this research in collaboration. J.F. and L.Z. have an experiment and manage the experimental data, H.W. and Z.C. proposed the project support, Y.X. proposed the analysis method, and H.D. provided substantial help with the paper schedule. All authors have read and agreed to the published version of the manuscript.

Funding: The authors gratefully acknowledge the financial support for this work provided by the National Natural Science Foundation of China (51974087, 51904074), Anhui Provincial Key Research and Development Planning Foundation (202004a07020019, 202004a07020049), Anhui Provincial Natural Science Foundation (1908085QE203), and Anhui Jianzhu University Science Research Foundation (2020QDZ02).

Institutional Review Board Statement: Not applicable.

Informed Consent Statement: Not applicable.

Data Availability Statement: The data presented in this study are available on request from the corresponding author.

Conflicts of Interest: The authors declare no conflict of interest.

Nomenclature

A, B	Correlation coefficients
d	Sieved particle diameter (m)
d_p	particle equivalent diameter (m)
D	Inner diameter of experimental cylinder (m)
Eu	Euler number
f_p	Friction factor
H	Measured bed layer height (m)
r	Actual distance between measured point and bed layer center (m)
R	Radius of bed layer
Re	Reynolds number, $\rho u d_p/\mu$
T_0	Ambient temperature (K)
u	Air superficial velocity (m/s)
BL	bed layer
FPD	flow pressure drop
SVT	sinter vertical tank
Greek symbols	
ΔP	Pressure drop of air flow (Pa)
$\Delta P/H$	Pressure drop per unit height (Pa/m)
μ	Dynamic viscosity (Pa·s)
ε	Bed layer voidage
ρ	Air density (kg/m^3)
Φ	Particle sphericity
Subscripts	
cal	Calculation value
exp	Experimental value
p	Particle

References

1. Barton, N.G. Simulations of air-blown thermal storage in a rock bed. *Appl. Therm. Eng.* **2013**, *55*, 43–50. [CrossRef]
2. Bansal, P.; Jain, S.; Moon, C. Performance comparison of an adiabatic and an internally cooled structured packed-bed dehumidifier. *Appl. Therm. Eng.* **2011**, *31*, 14–19. [CrossRef]
3. Bindra, H.; Bueno, P.; Morris, J.F.; Shinnar, R. Thermal analysis and exergy evaluation of packed bed thermal storage systems. *Appl. Therm. Eng.* **2013**, *52*, 255–263. [CrossRef]
4. Calis, H.P.A.; Nijenhuis, J.; Paikert, B.C.; Dautzenberg, F.M.; Bleek, C.M.V.D. CFD modelling and experimental validation of pressure drop and flow profile in a novel structured catalytic reactor packing. *Chem. Eng. Sci.* **2001**, *56*, 1713–1720. [CrossRef]
5. Cai, J.J.; Dong, H. Method and Device of Sinter Waste Heat Recovery and Utilization with Vertical Tank. Chinese Patent 200910187381.8, 5 January 2011.
6. Dong, H.; Li, L.; Liu, W.J.; Wang, B.; Suo, Y.S.; Cai, J.J. Process of waste heat recovery and utilization for sinter in vertical tank. *China Metall.* **2012**, *22*, 6–11.
7. Dong, H.; Zhao, Y.; Cai, J.J.; Zhou, J.W.; Ma, G.Y. On the air leakage problem in sintering cooling system. *Iron Steel* **2012**, *47*, 95–99.
8. Montillet, A. Flow through a finite packed bed of spheres. *J. Fluid Eng.* **2004**, *126*, 139–143. [CrossRef]
9. Çarpinlioglu, M.Ö.; Özahi, E.; Gündogdu, M.Y. Determination of laminar and turbulent flow ranges through vertical packed beds in terms of particle friction factors. *Adv. Powder Technol.* **2009**, *20*, 515–520. [CrossRef]
10. Yang, J.; Wang, Q.W.; Bu, S.S.; Zeng, M.; Wang, Q.W.; Nakayama, A. Experimental analysis of forced convective heat transfer in structured packed beds with spherical or ellipsoildal particles. *Chem. Eng. Sci.* **2012**, *71*, 126–137. [CrossRef]
11. Allen, K.G.; Backström, T.W.; Kröger, D.G. Packed bed pressure drop dependence on particle shape, size distribution, packing arrangement and roughness. *Powder Technol.* **2013**, *246*, 590–600. [CrossRef]
12. Bu, S.S.; Yang, J.; Li, S.Y.; Wang, Q.W. Effects of point contact treatment methods on flow and heat transfer of structured packed beds. *J. Eng. Thermophys.* **2013**, *34*, 534–537.
13. Pistocchini, L.; Garone, S.; Motta, M. Porosity and pressure drop in packed beds of spheres between narrow parallel walls. *Chem. Eng. J.* **2016**, *284*, 802–811. [CrossRef]
14. Tian, X.W.; Xu, S.M.; Sun, Z.H.; Wang, P.; Xu, L.; Zhang, Z. Experimental study on flow and heat transfer of power law fluid in structured packed porous media of particles. *Exp. Therm. Fluid Sci.* **2018**, *90*, 37–47. [CrossRef]
15. Guo, Z.H.; Sun, Z.N.; Zhang, N.; Ding, M.; Liu, J.Q. Pressure drop in slender packed beds with novel packing arrangement. *Powder Technol.* **2017**, *321*, 286–292. [CrossRef]

16. Halkarni, S.S.; Sridharan, A.; Prabhu, S.V. Influence of inserts on the pressure drop distribution in randomly packed beds with uniform sized spheres in the endshield model of AHWR. *Exp. Therm. Fluid Sci.* **2016**, *74*, 181–194. [CrossRef]
17. Baghapour, B.; Rouhani, M.; Sharafian, A.; Kalhori, S.B.; Bahrami, M. A pressure drop study for packed bed adsorption thermal energy storage. *Appl. Therm. Eng.* **2018**, *138*, 731–739. [CrossRef]
18. Toit, C.G.; Loggerenberg, P.J.; Vermaak, H.J. An evaluation of selected friction factor correlations and results for the pressure drop through random and structured packed beds of uniform spheres. *Nucl. Eng. Des.* **2021**, *379*, 111213. [CrossRef]
19. Ergun, S. Fluid flow through packed columns. *Chem. Eng. Prog.* **1952**, *48*, 89–94.
20. Macdonald, I.; El-Sayed, M.; Mow, K.; Dullien, F. Flow through porous media-the Ergun equation revisited. *Ind. Eng. Chem. Fundam.* **1979**, *18*, 199–208. [CrossRef]
21. Comiti, J.; Renaud, M. A new model for determining mean structure parameters of fixed beds from pressure drop measurements: Application to beds packed with parallelepipedal particles. *Chem. Eng. Sci.* **1989**, *44*, 1539–1545. [CrossRef]
22. Özahi, E.; Gündogdu, M.Y.; Çarpınlıoglu, M.Ö. A modification on Ergun's correlation for use in cylindrical packed beds with non-spherical particles. *Adv. Powder Technol.* **2008**, *19*, 369–381. [CrossRef]
23. Dukhan, N.; Bağcı, Ö.; Özdemir, M. Experimental flow in various porous media and reconciliation of Forchheimer and Ergun relations. *Exp. Therm. Fluid Sci.* **2014**, *57*, 425–433. [CrossRef]
24. Amiri, L.; Ghoreishi-Madiseh, S.A.; Hassani, F.P.; Sasmito, A.P. Estimating pressure drop and Ergun/Forchheimer parameters of flow through packed bed of spheres with large particle diameters. *Powder Technol.* **2019**, *356*, 310–324. [CrossRef]
25. Kürten, H.; Raasch, J.; Rumpf, H. Beschleunigung eines kugelförmigen Feststoffteilchens im Strömungsfall konstanter Geschwindigkeit. *Chem. Eng. Technol.* **1966**, *38*, 941–948.
26. Hicks, R.E. Pressure drop in packed beds of spheres. *Ind. Eng. Chem. Fundam.* **1970**, *9*, 500–502. [CrossRef]
27. Tallmadge, J.A. Porosity and pressure drop—An extension to higher Reynolds numbers. *AIChE J.* **1970**, *16*, 1092–1093. [CrossRef]
28. Lee, J.S.; Ogawa, K. Pressure drop through packed beds. *J. Chem. Eng. Jpn.* **1974**, *27*, 691–693. [CrossRef]
29. Montillet, A.; Akkari, E.; Comiti, J. About a correlating equation for predicting pressure drops through packed beds of spheres in a large range of Reynolds numbers. *Chem. Eng. Process.* **2007**, *46*, 329–333. [CrossRef]
30. Çarpinlioğlu, M.Ö.; Özahi, E. A simplified correlation for fixed bed pressure drop. *Powder Technol.* **2008**, *187*, 94–101. [CrossRef]
31. Li, X.Z.; Zhu, D.S.; Yin, Y.D.; Liu, S.J.; Mo, X. Experimental study on heat transfer and pressure drop of twisted oval tube bundle in cross flow. *Exp. Therm. Fluid Sci.* **2018**, *99*, 251–258. [CrossRef]
32. Li, X.Z.; Zhu, D.S.; Sun, J.F.; Mo, X.; Yin, Y.D. Air side heat transfer and pressure drop of H type fin and tube bundles with in line layouts. *Exp. Therm. Fluid Sci.* **2018**, *96*, 146–153. [CrossRef]
33. Sun, X.Y.; Dai, Y.J.; Ge, T.S.; Zhao, Y.; Wang, R.Z. Comparison of performance characteristics of desiccant coated air-water heat exchanger with conventional air-water heat exchanger-Experimental and analytical investigation. *Energy* **2017**, *137*, 399–411. [CrossRef]
34. Feng, J.S.; Dong, H.; Dong, H.D. Modification of Ergun's correlation in vertical tank for sinter waste heat recovery. *Powder Technol.* **2015**, *280*, 89–93. [CrossRef]
35. Geldart, D. Estimation of basic particle properties for use in fluid-particle process calculations. *Powder Technol.* **1990**, *60*, 1–13. [CrossRef]
36. Feng, J.S.; Dong, H.; Cao, Z.; Wang, A.H. Voidage distribution properties of bed layer in sinter vertical tank. *J. Cent. South Univ. Sci. Technol.* **2016**, *47*, 8–13.